PHYSICAL REVIEW B **88**, 121409(R) (2013)

Strong magnetoelectric coupling in multiferroic Co/$BaTiO_3$ thin films

N. Jedrecy,[1,*] H. J. von Bardeleben,[1] V. Badjeck,[1] D. Demaille,[1] D. Stanescu,[2] H. Magnan,[2] and A. Barbier[2]
[1]*Institut des Nano Sciences de Paris, UPMC-Sorbonne Universités, CNRS-UMR7588, 4 Place Jussieu, 75252 Paris Cedex 05, France*
[2]*CEA, IRAMIS, SPCSI, F-91191 Gif-sur-Yvette Cedex, France*
(Received 24 July 2013; published 23 September 2013)

We have found evidence for a strong magnetoelectric (ME) coupling at room temperature between polycrystalline Co layers (5−40 nm) and single-crystalline (001)-oriented $BaTiO_3$ layers (15−17 nm). We took advantage of the quasi-single polarization orientation, perpendicular to the film plane, of the ferroelectric $BaTiO_3$ domains in the tetragonal phase. Using ferromagnetic resonance spectroscopy with the Co magnetization aligned either parallel or antiparallel to the $BaTiO_3$ polarization, we assessed a strong anisotropy of about 0.14 T in the Co resonance field positions, indicating a coupling constant of 0.27 s/F. When sweeping the temperature through the phase transitions of $BaTiO_3$, the two resonance positions are shifted in opposite directions. The ME coupling induces a notable magnetic anisotropy resulting in high values of the out-of-plane remanent magnetization. Our results are promising for future multiferroic devices.

DOI: 10.1103/PhysRevB.88.121409 PACS number(s): 75.85.+t, 07.57.Pt, 68.37.−d, 75.70.−i

Multiferroic structures involving ferromagnetic and ferroelectric orders are key elements for the development of novel memory and logic devices with low energy consumption and nanometer-ranged sizes.[1–3] Single phase multiferroics with ordering temperatures above 300 K are rare since insulating behavior and cooperative cation off-centering required for ferroelectricity are antagonist to parallel magnetic spin ordering.[4] Artificial composite multiferroic systems are an alternative that received renewed attention recently.[5–9] In particular, they promise relevant functionalities, among which the manipulation of magnetization by use of an electrical voltage instead of a magnetic field, through switching of electric polarization.[8,9] This requires a strong and well-understood magnetoelectric coupling between the ferromagnetic (FM) and ferroelectric (FE) components. In spite of the tremendous research effort, the fundamental physics behind magnetoelectric interactions remains puzzling in many aspects.[10]

Most works on FM/FE systems have been carried out using FE (e.g., $BaTiO_3$) bulk crystals.[11–16] Although adequate to show evidence of interactions between FE and FM phases, this situation is hardly of any help when considering nanometer-sized systems. The intrinsic electric properties of a FE macroscopic crystal are likely to be different from those of the thin film counterpart.[17,18] The transposition of coupling phenomena should thus be considered with care. In particular, a FE crystal generally consists of domains with different polarization orientations, each of which may exert a different influence on the overlying FM film.[19] Moreover, when applying electric fields to a FE crystal, magnetoelastic effects may overcome purely magnetoelectric effects, because of large piezoelectric distortions.

Here we have found evidence by ferromagnetic resonance spectroscopy that a strong magnetoelectric coupling exists in a system where both FM and FE are thin films: Co (5–40 nm)/$BaTiO_3$ (17 nm) layers grown on $SrTiO_3$(001) substrates. The epitaxial $BaTiO_3$ layers at room temperature have a (quasi) single out-of-plane polarization state that allows using them as a ferroelectric reference state. Depending on whether the magnetization vector of Co is aligned parallel or antiparallel to the electric polarization vector of $BaTiO_3$, distinct Co ferromagnetic resonance fields are measured at 300 K. These resonance fields shift oppositely upon cooling/heating through the phase transitions of $BaTiO_3$. On the contrary, no shift at all is observed when the magnetization is perpendicular to the polarization.

The 15–17-nm-thick ferroelectric $BaTiO_3$ (BTO) layers were grown by atomic oxygen assisted molecular beam epitaxy. Details on the growth process and on the high crystalline quality/stoichiometry of our BTO (001) films are given in Ref. 20. At room temperature, for thicknesses above 10 nm, the BTO layers adopt the perovskite-derived tetragonal structure with lattice parameters close to the bulk ones: $a = 3.99$ Å, $c = 4.04$ Å. Atomic force microscopy [Fig. 1(a)] shows that the final surface exhibits 100–150-nm-wide flat terraces (mean roughness = 0.2 nm) with unit-cell steps decorated by Ba-rich oxide three-dimensional (3D) clusters/lines. Piezoresponse force microscopy (PFM) reveals [Fig. 1(b)] that at 300 K the electric polarization of the as-grown film is almost entirely out of plane with ≈90% of the domains polarized outwards along the c axis. The polarization may easily be reversed by use of small voltages (2–4 V) between the tip and the Nb-doped $SrTiO_3$ substrate. Figure 1(b) shows a circle of 0.7 μm diameter along which the polarization has been switched downwards after poling by use of the tip.

Ferromagnetic Co films with thicknesses equal to 5, 15, and 40 nm were deposited *in situ* in ultrahigh-vacuum conditions on BTO/$SrTiO_3$(001) at room temperature, keeping the nominal BTO thickness between 15 and 17 nm. The films were capped with ≈6 nm Au to avoid *ex situ* Co oxidation. One of the Co thicknesses investigated was reproduced twice in order to cross-check the results. Typical reflection high-energy electron diffraction (RHEED) patterns are shown in Fig. 1(c). The rings in the RHEED diagram of Co reveal the polycrystalline nature of the Co film; the presence of some preferentially orientated grains is suggested by some additional 3D spots. The x-ray reflectivity curve related to the thicker Co film is displayed in Fig. 1(d). The fit shows that the interface between BTO and Co is sharp with a roughness lower than 0.7 nm. Considering an eventual formation of CoO at the interface did not improve the fit. The Co film is continuous as confirmed by high resolution

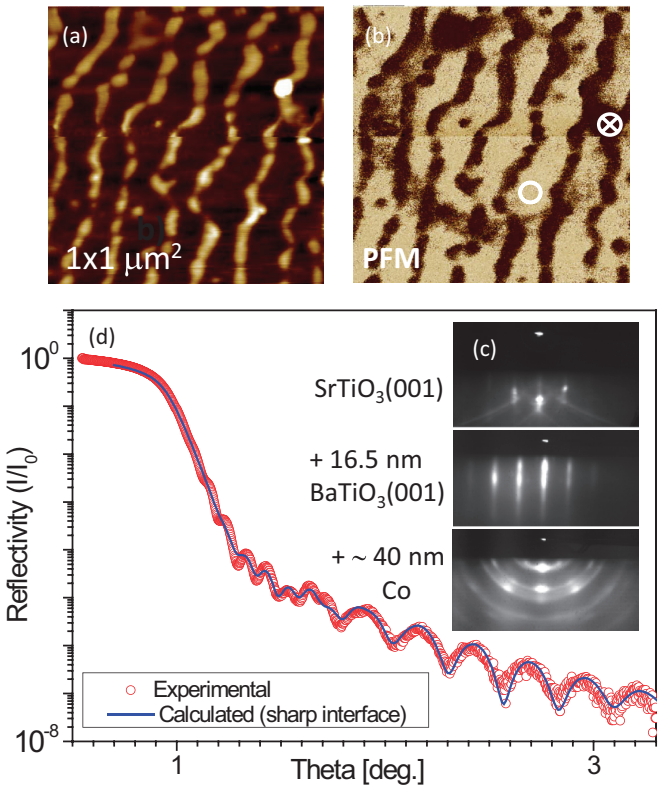

FIG. 1. (Color online) (a), (b) Typical topographic (a) and phase (b) PFM 1 × 1 μm^2 images obtained *ex situ* from a 20-nm-thick BTO film after 4 V poling along a circle of 0.7 μm diameter. (c) Typical RHEED patterns obtained after 17 nm of BTO, and then 40 nm of Co have been deposited on the $SrTiO_3$ substrate. (d) Experimental x-ray reflectivity curve simulated using a sharp interface system: Au (5.2 nm)/Co (38.2 nm)/BTO (16.5 nm)/$SrTiO_3$ with surface/interface roughness of 2.9, 1.4, 0.7, and 0.2 nm, respectively.

transmission electron microscopy (HRTEM) (Fig. 2). Some hcp Co grains with their c axis along the in-plane $[100]_{BTO}$ axis are identified in the image zooms.

The magnetic properties have first been studied by superconducting quantum interference device (SQUID) and/or vibrating-sample magnetometry (VSM). The raw signals were corrected for the diamagnetic contribution of the substrate. The magnetization M of the thicker Co film (40 nm) measured at 300 K as a function of an external field μ_0 H is shown in Fig. 3(a) with the field in the surface plane (IP) or out of the surface plane (OP). The IP hysteresis loop is as expected from polycrystalline hcp Co with a saturation magnetization ($M_s = 1.43 \times 10^6$ A m^{-1}) consistent with that of bulk crystals, a remanent magnetization M_r almost equal to M_s ($M_r = 0.85 M_s$), and a small coercive field ($\mu_0 H_{c_{IP}} =$ 1 mT). The OP hysteresis loop reveals a rather high remanent magnetization M_r value about 15% of M_s and for moderate field values $0 \leqslant \mu_0 H \leqslant 0.7$ T, a magnetization standing between 15% and 60% of saturation. Similar OP M-H curves were measured for the 15- [inset Fig. 3(a)] and 5-nm-thick Co films. This OP magnetization behavior is unexpected from continuous polycrystalline thin films for which shape anisotropy should align magnetization in the plane of the film in low magnetic field conditions.[21,22] The OP M-H curves of our Co/BTO layers are close to that reported for 40-nm-thick hcp (0001)-textured Co layers grown on Al_2O_3(0001) and where the magnetocrystalline anisotropy (MCA) acts in favor of a magnetization along the Co c axis, and thus along the OP z direction.[22] In our case, since we deal with polycrystalline Co thin films, the MCA averaged on all grains contributes negligibly. Therefore, the only explanation for the OP behavior is that the Co/BTO interface plays a major role; in other words, that the BTO layers are responsible for the magnetic perpendicular anisotropy. Figure 3(b) shows

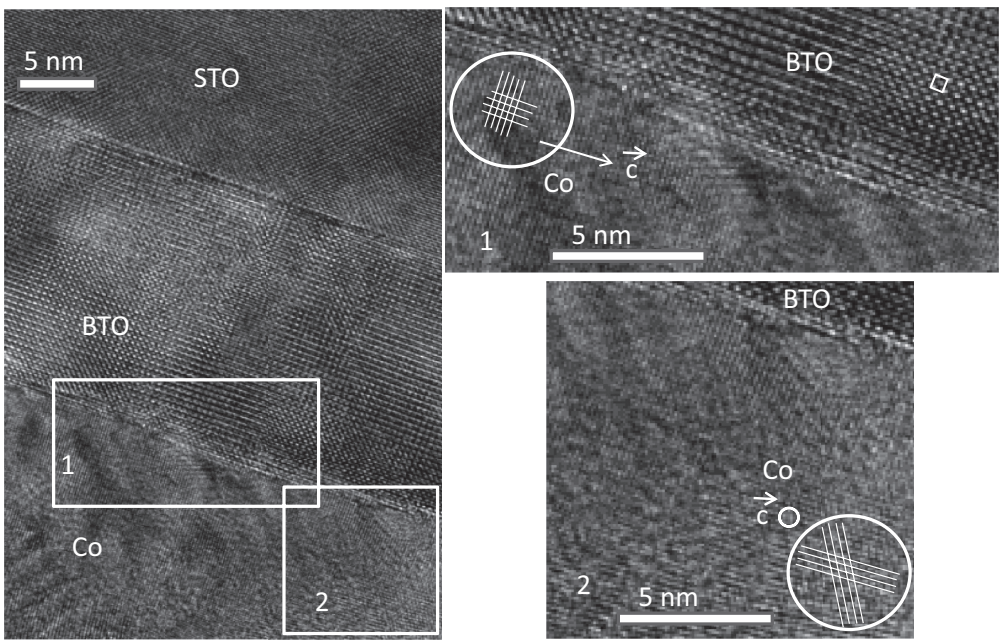

FIG. 2. HRTEM image of the Au (10 nm)/Co (40 nm)/BTO (17 nm) system, with zooms showing hcp Co grains with different epitaxial relationships with respect to BTO.

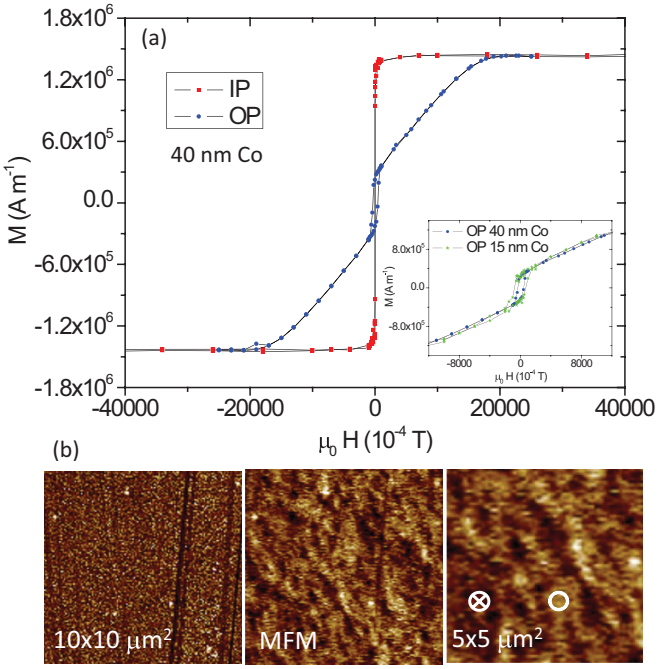

FIG. 3. (Color online) (a) Hysteresis loops measured at 300 K of a 40-nm-thick Co film deposited on a 17 nm BTO film in the in-plane (IP) and out-of-plane (OP) configurations. The inset shows that the OP signal from the 15 nm Co film is similar to that of the 40 nm film. (b) Topographic (left) and MFM images (middle and right) of the Au (10 nm)/Co (40 nm)/BTO (17 nm) system, after the sample has been magnetized OP.

images obtained by magnetic force microscopy (MFM) on the Au(6 nm)/Co(40 nm)/BTO(17 nm) system at the OP remanence. The topographic image is as expected from a rough Au surface with 3D clustering. The magnetic domains in the MFM image appear in the form of stripes with alternating dark and bright contrast (domains with up and down magnetization), irregularly aligned at ≈45° of the $[100]_{BTO}$ direction. The stripe pattern closely resembles that observed on (0001)-textured Co films.[22] It derives from the minimization of the magnetic free energy by means of antiparallel alignment of OP magnetized domains.

Since the Curie temperature of Co is ≈1400 K, any change of the magnetization with the temperature T could be related to magnetostriction effects through BTO lattice distortions with respect to the parent perovskite cubic structure: Starting from the tetragonal phase at $T = 300$ K and decreasing the temperature, a first transition occurs at 278 K towards an orthorhombic phase, a second one at 183 K towards a rhombohedral structure. Importantly, for a single crystalline (001) BTO crystal, the electric polarization switches from [001] to ⟨101⟩ or ⟨111⟩ direction, respectively, and the perpendicular component of the electric polarization decreases with abrupt jumps. The situation for thin BTO films is more complex. The critical temperatures and the polarization states of the different phases may be modified by the strain induced by the substrate, the thermal expansion mismatch between the film and the substrate, or the reduced-size effects.[23–27] At 300 K, our (001)-oriented BTO films are unstrained, have the tetragonal structure, and exhibit a polarization essentially

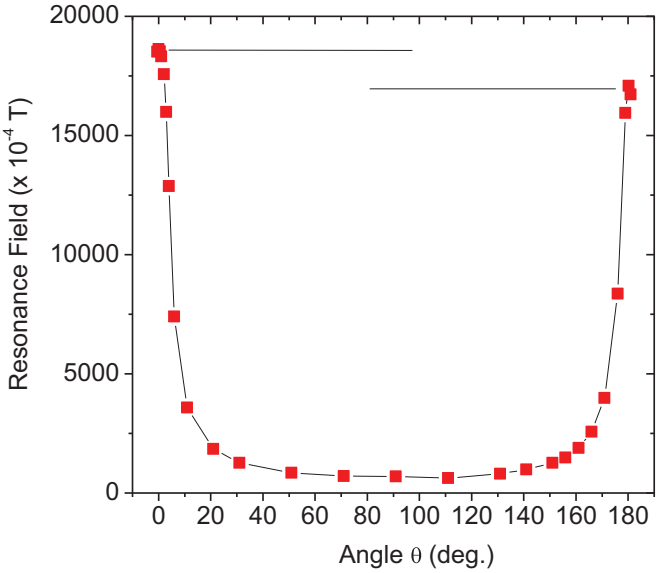

FIG. 4. (Color online) FMR resonance magnetic field values measured at room temperature as a function of the angle θ between the magnetic field and the sample normal axis for the 40-nm-thick Co film on BTO (17 nm).

parallel to [001]. Hysteresis M-H loops measured with the thicker film in the IP geometry did produce jumps of M_r and M_s at temperatures close to those of the rhombohedral-orthorhombic and orthorhombic-tetragonal phase transitions. However, the weak magnitude (≈1.5%) of these jumps makes any quantitative analysis difficult. Magnetization measurements in the OP geometry are problematic since the OP remanent magnetization is worth only 15% of the saturation value due to the presence of up and down domains.

The magnetic response was thus investigated by using a more direct and sensitive technique, which is ferromagnetic resonance (FMR) spectroscopy. Here, a microwave radiation ($\nu \approx 9.5$ GHz) is absorbed by the Co film at specific resonance magnetic fields H_{res} which depend on the experimental geometry. Figure 4 shows the angular variation of the resonance field for the Co(40 nm)/BTO(17 nm) film when varying the angle θ between the external applied magnetic field and the normal z axis of the sample, from 0° to 180°. The large shift of the resonance field between 0° and 90° can be simulated on the basis of the Kittel formula. For $\theta = 0$ (or π), the resonance field H_{res} is given by

$$\mu_0 H_{res} = h\nu/(g_{Co}\mu_B) + \mu_0 M, \quad (1)$$

while for $\theta = \pi/2$, it is given by

$$[h\nu/(g_{Co}\mu_B)]^2 = [\mu_0 H_{res} + \mu_0 M]\,\mu_0 H_{res} \quad (2)$$

with $g_{Co} = 2.18$. Equations (1) and (2) consider only demagnetization field effects due to the thin film shape anisotropy through the $(\mu_0 M)$ term which is very large (≈17 500 × 10^{-4} T). In the case that MCA intervenes, the $(\mu_0 M)$ term in (1) should be replaced by an effective value $(\mu_0 M_{eff}) = (\mu_0 M - 2K_{eff}/M)$. Due to the polycrystalline nature of our Co film, the average on the differently oriented grains makes the $(\mu_0 M_{eff})$ term moderately reduced with respect to $(\mu_0 M)$. Unexpectedly, a noticeable asymmetry is detected in

the resonance curve of Fig. 4 comparing the behavior at 0° and 180°, respectively. The same measurements performed with a polycrystalline Co film of equivalent thickness on top of a TiO_2/Si(001) substrate have led to a perfectly symmetric resonance curve. The asymmetric resonance field values in the OP geometry are explained according to the modified formula (see Ref. 28) with respect to (1) which includes a magnetoelectric coupling term:

$$\mu_0 H_{\rm res} = h\nu/(g_{\rm Co}\,\mu_{\rm B}) + \mu_0 M_z - \left(2K\,M_z/M_s^2\right) + \lambda P_z, \quad (3)$$

where P_z is the OP BTO polarization, and λ stands for the coupling constant which appears in the interface magnetoelectric free energy ($+\lambda$ **MP**) of the system if any. The sign of P_z in (3) is defined with respect to magnetization: it is written $+P$ if **P** is parallel (‖) to **M**, and $-P$ if **P** is antiparallel (anti-‖) to **M**. Assuming that the BTO film has a single orientation of the polarization, in the case $\theta = 0°$, the magnetic field **H** is applied parallel to the BTO polarization **P**; in the case $\theta = 180°$, it is applied antiparallel. The high resonance fields in the OP geometry imply the magnetization is close to saturation ($M_z \approx M_s$). We thus test ‖ or anti-‖ alignments of the polarization **P** and magnetization **M** vectors, respectively. The shift of the resonance field in Fig. 4 by -1400×10^{-4} T at 180° with respect to that at 0° corresponds to ($2\lambda P$).

A series of FMR spectra measured at different temperatures T across the orthorhombic-tetragonal phase transition are displayed in Figs. 5(a) ($\theta = 180°$) and 5(b) ($\theta = 0°$), respectively. The derived values of the Co resonance field $\mu_0 H_{\rm res}$ are plotted as a function of T in Figs. 5(c) and 5(d). Raising the temperature from 220 K, the resonance field $\mu_0 H_{\rm res}$ first slowly decreases in each geometry with the same slope, then from ≈260 up to 290 K markedly shifts to lower or higher values depending on the geometry: The shifts are -850×10^{-4} T for **M** anti-‖ **P** and $+550 \times 10^{-4}$ T for **M**‖**P**. These shifts of $\mu_0 H_{\rm res}$ occur concomitantly to the BTO orthorhombic-tetragonal transition. Coming back from 310 to 220 K, one observes a small hysteresis in the $H_{\rm res}$-T curve [Fig. 5(d)]. The negative (positive) shift at ≈270 K for the field ***H*** antiparallel (parallel) to the BTO polarization **P** may solely be explained by the magnetoelectric $\lambda P_z = \pm\lambda P$ term in Eq. (3). The slow linear decrease of resonance positions as a function of T on both sides of the BTO phase transition is attributed to the weak MCA contribution which accordingly monotonously decreases with raising temperature. Note the same linear decrease with T has been measured for the reference Co/TiO_2/Si sample.

Our Co/BTO/$SrTiO_3$(001) sample is almost fully polarized OP, therefore, we should not observe any shift of the resonance field with temperature if the magnetization is in plane i.e., perpendicular to the electric polarization. Indeed, the FMR resonance spectra in the IP configuration do not shift at all in the 220–310 K temperature range [Figs. 5(e) and 5(f)].

In a BTO single crystal, the orientation of **P** varies from the [001] direction towards [101]-like directions at the tetragonal-orthorhombic transition. The configuration of electric polarization in our thin BTO film in the orthorhombic phase is unknown. We observe that the magnetic resonance fields in this phase do not depend on the orientation of the sample (0° or 180°) with respect to the magnetic field. From Eq. (3), we can conclude that, in this phase, we have an average $\langle P_z \rangle = 0$ (an equal number of domains with $\pm P_z$ polarization, or a nonferroelectric phase). With this assumption, retaining an average value of $\pm 700 \times 10^{-4}$ T for the (λP_z) coupling term and a polarization magnitude in the tetragonal phase equal to that of bulk BTO ($P_z = 26\ \mu$C/cm^2), we derive a λ coupling value equal to 0.27 s/F, in good agreement with the theoretical

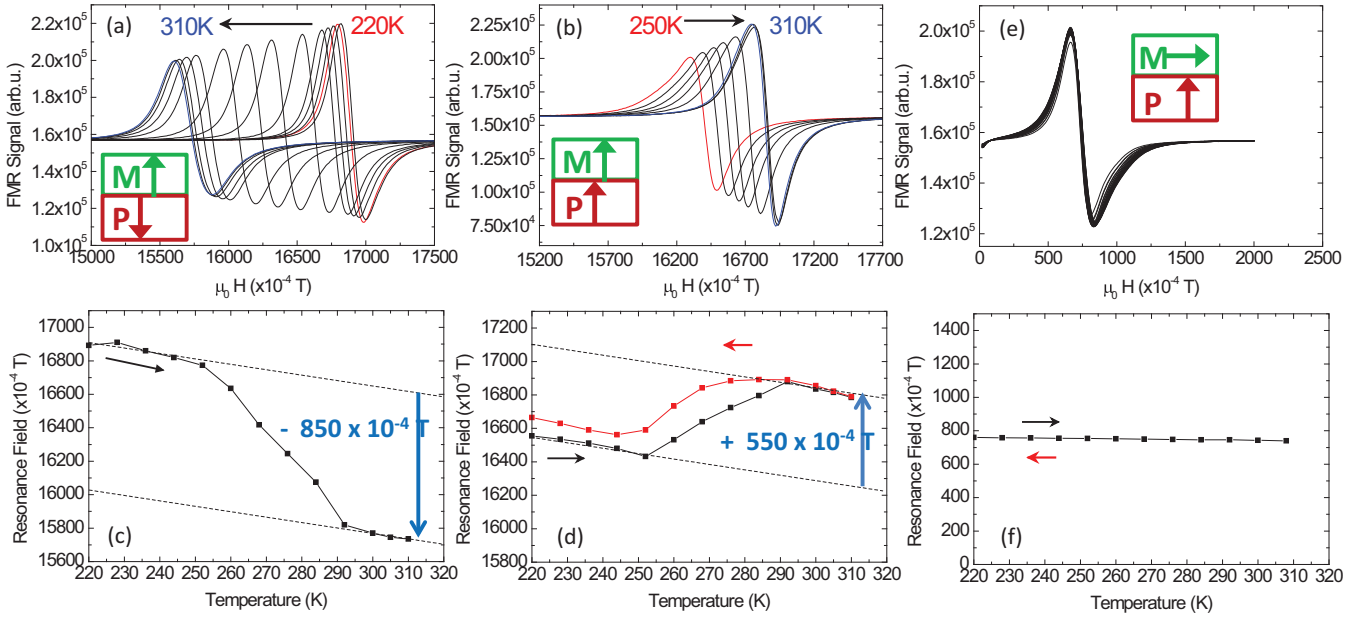

FIG. 5. (Color online) (a), (b) FMR spectra of the 40-nm-thick Co/BTO film in the OP configuration collected at different temperatures from 220 to 310 K, with the magnetic field H applied either (a) antiparallel or (b) parallel to the BTO polarization P, respectively. (c), (d) Resonance field values as a function of temperature in the two configurations: (c) M anti-‖ P and (d) M ‖ P. (e), (f) FMR spectra in the IP configuration and related resonance field as a function of temperature.

prediction of Sukhov *et al*.[28] The (λP_z) value is of the same order of magnitude as the $\mu_0\ \Delta M$ change with polarization orientation calculated by Duan *et al*. for the Fe/BTO system.[29] Importantly, we have checked that the shifting of the resonance field between the two 0° and 180° orientations disappears when increasing the temperature from 300 to 390 K where the BTO layers transform into the paraelectric ($P_z = 0$) cubic phase.

The Co/BTO magnetoelectric coupling can explain the rather high value of OP M_r/M_s at room temperature. The OP magnetization could be favored by the OP electric polarization via an anisotropy term in the energy.[30]

In summary, a strong magnetoelectric coupling has been demonstrated on a FM/FE nanometer-thick system: Co/$BaTiO_3$ grown on $SrTiO_3$(001). This coupling is unambiguously determined through the ferromagnetic resonance behavior of Co. At 300 K, ∥ and anti-∥ alignments of $BaTiO_3$ polarization and Co magnetization produce distinct resonance field values. These resonance positions shift oppositely at the structural phase transitions (≈278 and ≈390 K) of the BTO film. Last, the coupling induces a significant out-of-plane remanent magnetization of the FM film in the 5−40 nm thickness range.

N.J. warmly thanks M. Escudier and M. Jacquet (INSP) for their skillfull work on crystals, as well as Y. Li (IPCM) and Y. Klein (IMPMC) for their maintenance work on the SQUID and VSM apparatus. We also wish to thank E. Lacaze and S. Hidki for technical assistance in connection with the MFM and x-ray experiments. The PFM measurements were done on a BRUKER ICON microscope with the help of P. De Wolf. This work was partly supported by the CNano-MAEBA grant.

*jedrecy@insp.jussieu.fr

[1] R. Ramesh and Nicola A. Spaldin, Nat. Mater. **6**, 21 (2007).
[2] Y.-H. Chu *et al*., Nat. Mater. **7**, 478 (2008).
[3] S. H. Baek *et al*., Nat. Mater. **9**, 309 (2010).
[4] W. Eerenstein, N. D. Mathur, and J. F. Scott, Nature (London) **442**, 759 (2006).
[5] T. N. Narayanan, B. P. Mandal, A. K. Tyagi, A. Kumarasiri, X. Zhan, M. G. Hahm, M. R. Anantharaman, G. Lawes, and P. M. Ajayan, Nano Lett. **12**, 3025 (2012).
[6] L. Bocher *et al*., Nano Lett. **12**, 376 (2012).
[7] C. A. F. Vaz, J. Hoffman, C. H. Ahn, and R. Ramesh, Adv. Mater. **22**, 2900 (2010).
[8] D. Pantel, S. Goetze, D. Hesse, and M. Alexe, Nat. Mater. **11**, 289 (2012).
[9] S. M. Wu, S. A. Cybart, D. Yi, J. M. Parker, R. Ramesh, and R. C. Dynes, Phys. Rev. Lett. **110**, 067202 (2013).
[10] C. A. F. Vaz, J. Phys.: Condens. Matter **24**, 333201 (2012).
[11] H. F. Tian, T. L. Qu, L. B. Luo, J. J. Yang, S. M. Guo, H. Y. Zhang, Y. G. Zhao, and J. Q. Li, Appl. Phys. Lett. **92**, 063507 (2008).
[12] Y. Shirahata, T. Nozaki, G. Venkataiah, H. Taniguchi, M. Itoh, and T. Taniyama, Appl. Phys. Lett. **99**, 022501 (2011).
[13] D. Dale, A. Fleet, J. D. Brock, and Y. Suzuki, Appl. Phys. Lett. **82**, 3725 (2003).
[14] S. Geprägs, A. Brandlmaier, M. Opel, R. Gross, and S. T. B. Goennenwein, Appl. Phys. Lett. **96**, 142509 (2010).
[15] R. V. Chopdekar and Y. Suzuki, Appl. Phys. Lett. **89**, 182506 (2006).
[16] S. Polisetty, W. Echtenkamp, K. Jones, X. He, S. Sahoo, and Ch. Binek, Phys. Rev. B **82**, 134419 (2010).
[17] K. J. Choi *et al*., Science **306**, 1005 (2004).
[18] Y. S. Kim, Appl. Phys. Lett. **86**, 102907 (2005).
[19] R.V. Chopdekar *et al*., Phys. Rev. B **86**, 014408 (2012).
[20] A. Barbier, C. Mocuta, D. Stanescu, P. Jegou, N. Jedrecy, and H. Magnan, J. Appl. Phys. **112**, 114116 (2012).
[21] M. Hehn, S. Padovani, K. Ounadjela, and J. P. Bucher, Phys. Rev. B **54**, 3428 (1996).
[22] J. Brandenburg, R. Hühne, L. Schultz, and V. Neu, Phys. Rev. B **79**, 054429 (2009).
[23] N. A. Pertsev, A. G. Zembilgotov, and A. K. Tagantsev, Phys. Rev. Lett. **80**, 1988 (1998).
[24] Y. L. Li and L. Q. Chen, Appl. Phys. Lett. **88**, 072905 (2006).
[25] F. He and B. O. Wells, Appl. Phys. Lett. **88**, 152908 (2006).
[26] D. Szwarcman, D. Vestler, and G. Markovich, ACS Nano **5**, 507 (2011).
[27] X. Lu, Y. Kim, S. Goetze, X. Li, S. Dong, P. Werner, M. Alexe, and D. Hesse, Nano Lett. **11**, 3202 (2011).
[28] A. Sukhov, P. P. Horley, C.-L. Jia, and J. Berakdar, J. Appl. Phys. **113**, 013908 (2013).
[29] C.-G. Duan, S. S. Jaswal, and E. Y. Tsymbal, Phys. Rev. Lett. **97**, 047201 (2006).
[30] Y. Chen, A. Yang, M. R. Paudel, S. Stadler, C. Vittoria, and V. G. Harris, Phys. Rev. B **83**, 104406 (2011).